


Article

A New Route to Upgrading the High-Phosphorus Oolitic Hematite Ore by Sodium Magnetization Roasting-Magnetic Separation-Acid and Alkaline Leaching Process

Jian Pan , Shenghu Lu, Siwei Li *, Deqing Zhu, Zhengqi Guo, Yue Shi and Tao Dong

School of Mineral Processing and Bioengineering, Central South University, Changsha 410083, China; pjcsu@csu.edu.cn (J.P.); lushenghu@csu.edu.cn (S.L.); dqzhu@csu.edu.cn (D.Z.); guozqcsu@csu.edu.cn (Z.G.); shiyue@csu.edu.cn (Y.S.); dongtao@csu.edu.cn (T.D.)

* Correspondence: swli@csu.edu.cn

Abstract: In this paper, an innovative method is proposed to upgrade iron and remove phosphorus from high-phosphorus oolitic hematite ore by the sodium magnetization roasting–magnetic separation–sulfuric acid and sodium hydroxide leaching process. The process parameters of sodium magnetization roasting, acid leaching, and alkaline leaching were optimized. The results show that by only adopting traditional magnetization roasting–magnetic separation, an iron ore concentrate containing 57.49% Fe and 1.4% P_2O_5 at an iron recovery rate of 87.5% and a dephosphorization rate of 34.27% was produced, indicating that it is difficult to effectively dephosphorize and upgrade iron by the conventional magnetization roasting–magnetic separation process. The obtained rough magnetic concentrates were then subjected to acid and alkaline leaching steps, and the final product, assayed at 64.11% iron and 0.097% P_2O_5 , was manufactured successfully. Moreover, the added NaOH could promote the mineral phase reconstruction of aluminum- and silica-bearing minerals during magnetization roasting and intensify the upgrading of iron as well as enhance the growth of iron grains.

Keywords: high-phosphorus oolitic hematite; magnetization roasting; acid leaching; alkaline leaching



Citation: Pan, J.; Lu, S.; Li, S.; Zhu, D.; Guo, Z.; Shi, Y.; Dong, T. A New Route to Upgrading the High-Phosphorus Oolitic Hematite Ore by Sodium Magnetization Roasting-Magnetic Separation-Acid and Alkaline Leaching Process. *Minerals* **2022**, *12*, 568. <https://doi.org/10.3390/min12050568>

Academic Editors: Kyoungkeun Yoo and Geoffrey S. Simate

Received: 8 March 2022

Accepted: 28 April 2022

Published: 30 April 2022

Publisher's Note: MDPI stays neutral with regard to jurisdictional claims in published maps and institutional affiliations.



Copyright: © 2022 by the authors. Licensee MDPI, Basel, Switzerland. This article is an open access article distributed under the terms and conditions of the Creative Commons Attribution (CC BY) license (<https://creativecommons.org/licenses/by/4.0/>).

1. Introduction

High-phosphorus oolitic hematite ore is a typical refractory iron ore that is widely distributed around the world. It has the characteristics of low iron grade (35–50%), high phosphorus content (0.4–1.8%), and fine dissemination [1–4], probably due to the difficulties in upgrading iron and removing phosphorus [5].

Phosphorus in oolitic hematite ore mainly occurs in the form of hydroxyapatite, fluorapatite, and chlorapatite, and as a result, it is difficult to remove by traditional beneficiation [6]. Therefore, the removal of phosphorus from oolitic iron ore has attracted increasing attention. Many research approaches have been reported in previous studies [7–11] including froth flotation, acid leaching, direct reduction, and so on. Nunes et al. reported that froth flotation could decrease phosphorus content from 0.82% to 0.37% in a Brazilian hematite ore with a Flotigam EDA (an amine type collector) dosage of 150 g/t [12]. Although froth flotation can achieve dephosphorization to some extent, it also has several disadvantages such as a large loss of iron resources and limited upgrade of the iron grade. Previous studies have demonstrated that acid leaching of high phosphorus-bearing iron ores can decrease the phosphorus content to less than 0.05%. Apart from the high cost, it also causes severe pollution problems [8,13–15]. Delvasto et al. adopted a bio-leaching process to remove phosphorus from iron ores, and the results showed that the dephosphorization rate could reach 80% with leaching for 21 days [16]. Similar results were obtained by Wang et al. [17]. Bio-leaching could obtain a higher dephosphorization rate, but the long leaching time and time-consuming preparation of bacteria restrict its application in

the iron ore industry [18]. Therefore, some studies have focused on direct reduction and magnetization roasting to remove phosphorus from the ores.

The coal-based direct reduction–wet magnetic separation process has been used to upgrade oolitic hematite ore in recent years [19–26]. In a study by Kokal et al., HPOHO (49.50% Fe and 0.75% P) was roasted at 900 °C for 20 min and the crude concentrate was leached after magnetic separation in 3% dilute sulfuric acid for 1 h. The phosphorus content could be reduced to less than 0.2% and the iron grade of the concentrate was 59.9% with an iron recovery of 97% [27]. Sun et al. noted that an iron concentrate with 89.63% Fe with an iron recovery of 96.21% was obtained from an oolitic hematite ore, assayed at 42.21% Fe and 1.31% P, under reduction at 1250 °C for 50 min. However, the dephosphorization rate was low, consistent with other studies [24]. Therefore, several additives have been used to improve the indices such as Na₂SO₄, Na₂CO₃, Ca(OH)₂, and Na₂B₄O₇·10H₂O [1,28]. Ionkov et al. found that the phosphorus level dropped from 0.71% to 0.05% and the iron level increased from 49.16% to 66% at an iron recovery rate of 92.43% when the ore was roasted with 10% NaOH and 8% coke at 900 °C for 1 h, and the concentrate after grinding, water leaching, and magnetic separation was leached with 10% sulfuric acid for 15 min [29]. Yu et al. adopted the combination of Ca(OH)₂ and Na₂CO₃ as an additive for the reduction of oolitic hematite ore at 1200 °C, and a directly reduced iron assayed at 93.28% Fe and 0.07% P was obtained with an iron recovery of 92.30%. Direct reduction is an efficient way to separate iron and phosphorus from oolitic hematite ore [23]. However, the amount of reductant required is very high and the reduction time is very long, resulting in a high energy consumption and operation cost.

Thus, a new method to enrich iron and remove phosphorus from oolitic hematite iron ore was proposed in this paper: the sodium magnetization roasting–wet magnetic separation–acid and alkaline leaching process. In this process, sodium hydroxide is used during roasting to improve the reduction in iron-bearing minerals and the removal of phosphorus.

2. Materials and Methods

2.1. Materials

The ore in this test was a high-phosphorus oolitic hematite ore (HPOHO) of the Ningxiang type collected from Guangxi Province, China, and its chemical composition is shown in Table 1. The content of total Fe and P₂O₅ was 49.41% and 2.13%, respectively, and the content of FeO was only 0.64%, indicating the presence of sparse magnetite. Its X-ray diffraction (XRD) pattern (Figure 1) showed that the main mineral phases were hematite (Fe₂O₃), and a small part of quartz (SiO₂). The occurrence of iron in HPOHO is listed in Table 2. Iron mainly occurs in the form of hematite. The microstructure of HPOHO was observed under a microscope, and the results are presented in Figure 2. Iron mainly exists in the form of hematite and goethite and is distributed together with chamosite and collophanite. They are wrapped around each other and closely embedded to form a concentric ring belt structure, and their particle size was less than 10 µm, indicating that it is very difficult to recover iron by traditional beneficiation processes.

Table 1. Chemical compositions of HPOHO (wt.%).

Elements	TFe	FeO	CaO	MgO	SiO ₂	Al ₂ O ₃	S	Sr	P ₂ O ₅	LOI
Content	49.41	0.64	2.70	0.10	14.52	5.61	0.13	0.46	2.13	2.48

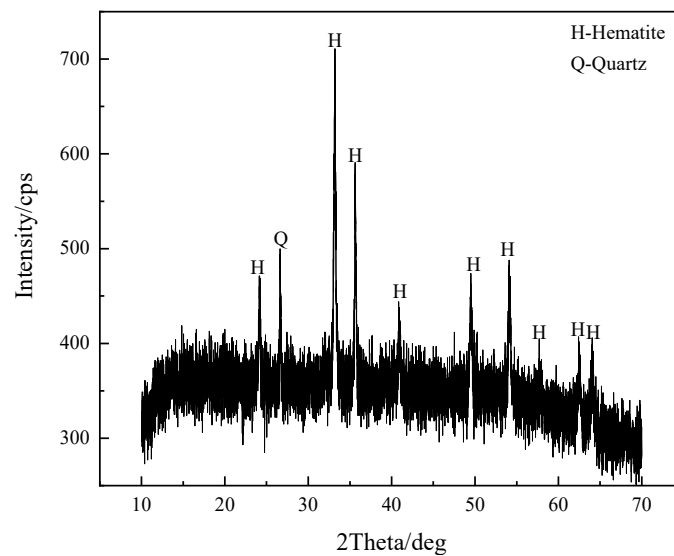


Figure 1. XRD pattern of HPOHO.

Table 2. Occurrence of iron in HPOHO.

Minerals	Hematite	Fayalite	Iron Sulfide	Iron Carbonate	Magnetite	TFe
Content	48.42	0.37	0.07	0.30	0.02	49.18
Iron distribution ratio	98.45	0.75	0.14	0.61	0.04	100

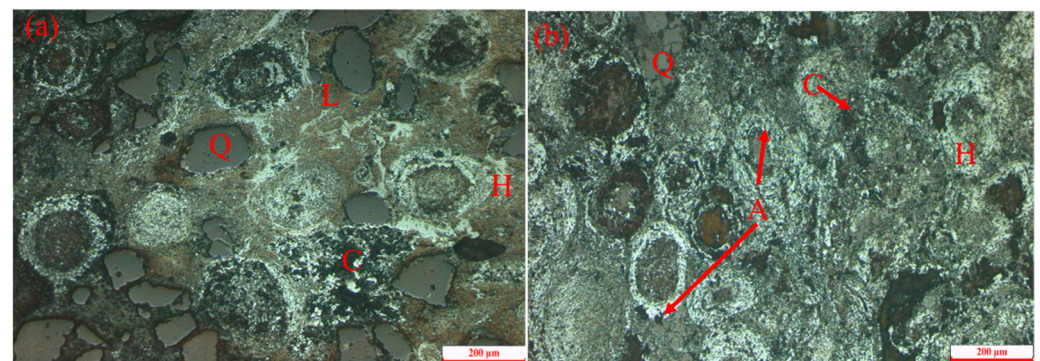


Figure 2. Microstructure of HPOHO (L: Goethite, H: Hematite, Q: Quartz, C: Chamosite, A: Apatite). (a,b) are the microstructure of HPOHO observed under a microscope.

Phosphorus mainly occurs in the form of collophanite; part of it is distributed with hematite layers to form an oolitic structure, and part of the granular apatite is dispersed between the oolitic structure. A SEM image of the oolitic structure is shown in Figure 3. It can be seen that phosphorus was distributed outside the oolitic and had a high degree of coincidence with calcium, and the morphology was granular, with a diameter between 5 and 20 μm , usually aggregated or distributed in a specific area between the oolitic. The phosphorus in the oolitic coexists with aluminum and strontium.

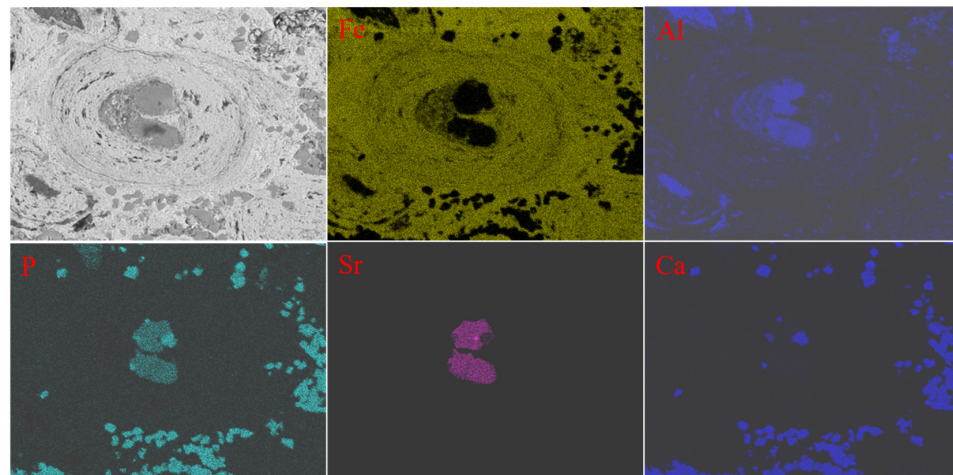


Figure 3. SEM of HPOH ore.

Bituminous coal was used as a reductant in this study, and its proximate analysis and the chemical composition of ash can be found in [30]. Analytical grade NaOH was used as an additive to promote and reconstruct the mineral phase of aluminum- and silica-bearing minerals during magnetization roasting.

2.2. Methods

A schematic flowchart for the upgrading process of HPOHO is presented in Figure 4 including the following steps: (1) magnetization roasting of HPOHO briquettes, followed by magnetic separation to upgrade Fe; and (2) an acid and alkaline leaching process to remove P.

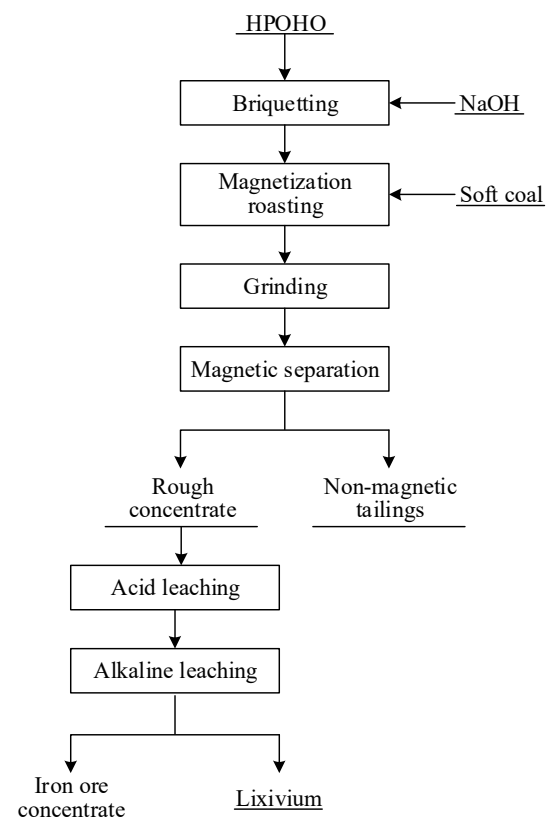


Figure 4. Experimental flowchart to upgrade the HPOHO.

2.2.1. Magnetization Roasting–Magnetic Separation

HPOHO was crushed and ground to more than 70% passing 74 μm . Then, the ore and additives were sufficiently mixed. The mixture was briquetted into cylinders (diameter 10 mm, height 10 mm) with a mass of 3 g containing 6% moisture, and then dried in a vacuum oven at 105 °C for 6 h until their weight did not change. Approximately 30 g of dry briquettes were loaded into a stainless-steel reaction tank. Soft coal was used to wrap the briquettes to provide a reducing atmosphere in the reactor [31]. When the shaft furnace (model: SK-12-13) reached the pre-set temperature, the tank was loaded into the furnace rapidly and then reduced for a certain time. After reducing, the stainless-steel reaction tank was taken out of the furnace and the reduced briquettes were cooled down to room temperature by water quenching.

The reduced briquettes were crushed to smaller than 1 mm, and then 20 g of crushed sample was mixed with 20 mL of water and ground in a small cone ball mill (model: XMQ 240 \times 90). Subsequently, the mixed slurry was loaded into a Davis tube (model: XCGS-73) to conduct the magnetic separation under a magnetic field strength of 1000 Gs. The rough magnetic iron ore concentrate was dried in a vacuum oven at 105 °C for 4 h. The roasting performance can be evaluated by using magnetic susceptibility and iron recovery, as shown in Equations (1) and (2):

$$\chi = \frac{TFe}{\omega(FeO)} \quad (1)$$

$$\varepsilon_1 = \frac{m_2 \times TFe_2}{m_1 \times TFe} \times 100\% \quad (2)$$

where ε_1 is the recovery rate of iron; TFe , $\omega(FeO)$, and TFe_2 are the content of iron and FeO in the roasted briquettes and rough iron concentrate, respectively; m_1 and m_2 are the mass of roasted briquettes (20 g) and rough iron concentrate, respectively; and χ is the magnetic susceptibility of roasted briquettes. The theoretic magnetic susceptibility of magnetite is 2.33; the closer the magnetic susceptibility value of the roasted ores to that value, and the better the beneficiation performance of the roasted ores.

The dephosphorization rate of every testing process was calculated as follows:

$$\eta_1 = \left(1 - \frac{m_2 \times x_2}{m_1 \times x_1} \right) \times 100\% \quad (3)$$

where η_1 is the dephosphorization rate; m_1 and m_2 are the weights of the sample before and after testing, respectively; and x_1 and x_2 are the contents of P_2O_5 of the sample before and after testing, respectively.

2.2.2. Acid and Alkaline Leaching

Phosphorus mainly occurs in the form of apatite in the roasted briquettes, which can be removed by acid leaching. The rough iron concentrate was acid leached at a pre-set temperature for a certain time and a fixed stirring speed. After leaching, the residue was washed with deionized water and dried until its weight did not change.

Considering that part of phosphorus compounds is insoluble in acid, alkaline leaching was adopted to treat the acid leaching residue. The alkaline leaching tests were performed in a 250 mL beaker, and the stirring speed was kept at 300 rpm. Finally, the solution was filtered to remove the phosphorus compound from the iron concentrate that was upgraded in the leaching residue.

2.3. Characterization of Materials

X-ray fluorescence spectroscopy (XRF, Axios mAX XRF Spectrometer, PANalytical B.V., Alemlo, Holland) with a rhodium target and operated at 60 kV and 160 mA in step mode with a 0.0001° step was used to measure the elemental content of the high-phosphorus oolitic hematite ore. Meanwhile, the contents of Fe and P were also determined by the chemical analysis method based on relevant standards (GB/T 6730.70-2013, GB/T

6730.18-2006) to verify the accuracy. The mineral compositions of iron were measured by chemical analysis based on the standard (GB/T6730.71-2014, GB/T 6730.77-2019). X-ray diffractometry (XRD, Simens D500 automatic X-ray diffractometer, Siemens AG, Berlin, Germany) with a copper target and operated at 40 kV and 250 mA in step mode with a 0.02° 2θ step and a count time of 0.5 s per step over a 2θ range from 10° to 80° was adopted to determine the phase compositions of high-phosphorus oolitic hematite ore. The XRD data were analyzed by the MDI Jade 6.5 software (ICDD, Newtown Square, PA, USA) via the quantification approach of Rietveld refinement. Scanning electron microscopy (SEM) images and energy dispersive spectroscopy (EDS, PhenomPro, Phenom-World, Eindhoven, The Netherlands) were used to observe the microstructure and reveal the distribution of elements in the raw mineral after the preparation of samples [32]. FactSage 7.0 (Thermfact/CRCT, Montreal, QC, Canada; GTT-Technologies, Herzogenrath, Germany) was used to calculate the standard Gibbs free energy change of the possible reactions during magnetization roasting.

3. Results and Discussion

3.1. Magnetization Roasting–Magnetic Separation Process

The effects of magnetization roasting parameters on the iron grade, iron recovery, and specific susceptibility of roasted briquettes are shown in Figure 5. Figure 5a shows that the iron grade increased from 56.74% to 57.21% with increasing magnetization roasting temperature from 750°C to 850°C . Meanwhile, iron recovery increased from 47.38% to 85.68%. Further increasing the temperature to 900°C , the iron recovery decreased to 78.55%. Magnetic susceptibility decreased from 2.6% to 1.8% with increased temperature from 750°C to 900°C . This is because roasted briquettes are over-reduced under roasting temperatures of 750°C and 800°C , indicating that a large amount of iron is reduced to metallic iron, resulting in increased iron recovery. At temperatures exceeding 850°C , the roasted briquettes are under-reduced, resulting in a decreased yield of magnetic separation concentrate, and therefore a decreased recovery rate. Magnetic susceptibility at 850°C was 2.26, which was closer to the theoretic magnetic susceptibility of magnetite (2.33), indicating a better performance of the roasted ores. From the above, the optimal magnetization roasting temperature was determined to be 850°C . At that temperature, the iron grade in magnetically separated ore was 57.21%, with a recovery rate of 85.68%.

Iron recovery increased from 75.39% to 85.43% when the duration was prolonged from 5 min to 13 min. When the time was increased further, the indices changed slightly. Meanwhile, magnetic susceptibility decreased from 3.37% to 2.39%. According to the magnetic susceptibility of roasted briquettes obtained at different magnetization times, it was found that the briquettes were over-reduced with 5 to 13 min of roasting time, resulting in increased iron recovery. When the duration was prolonged further, the roasted briquettes were under-reduced. In summary, 13 min is recommended as the optimal magnetization roasting time.

Iron recovery increased from 63.5% to 85.43% when the coal ratio was increased from 5% to 15%. Further increasing the ratio had a negative impact on iron recovery. Meanwhile, magnetic susceptibility decreased from 3.40% to 1.75% when the coal ratio was increased from 5% to 25%. According to the magnetic susceptibility of roasted briquettes obtained with coal ratios from 5% to 15%, it was found that the briquettes were over-reduced, indicating that the iron oxides were reduced to metallic iron. When the ratio was increased further, the magnetic susceptibility decreased, indicating that the FeO content in the roasted briquettes increased, resulting in decreased iron recovery. In summary, 15% is recommended as the optimal coal ratio.

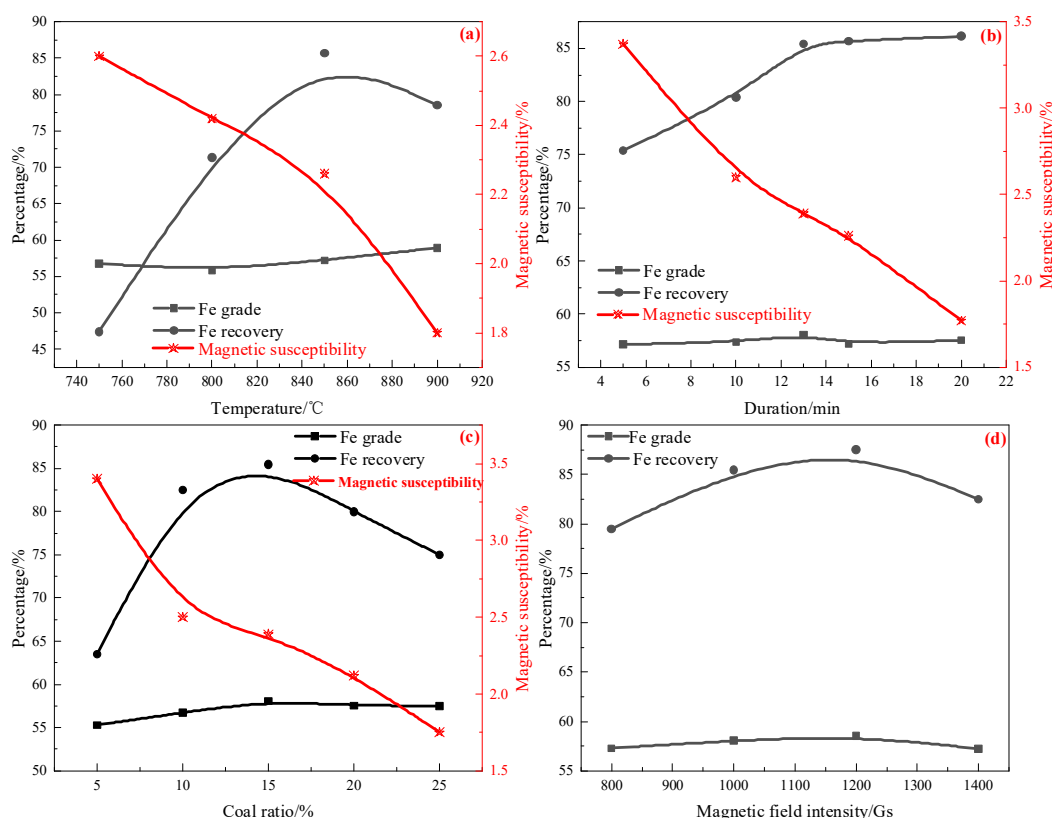


Figure 5. Effect of magnetization roasting parameters on iron grade, iron recovery, and specific susceptibility of roasted briquettes: (a) roasting duration of 15 min, magnetic field intensity of 1000 Gs; (b) roasting temperature of 850 °C, magnetic field intensity of 1000 Gs; (c) roasting temperature of 850 °C for 13 min, magnetic field intensity of 1000 Gs; (d) roasting at 850 °C for 13 min, grinding fineness of 80% less than 0.045 mm.

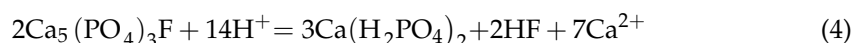
Increasing the magnetic field intensity had a slight impact on the iron grade. However, iron recovery increased from 79.5% to 87.5% when the magnetic field intensity was increased from 800 Gs to 1200 Gs. Further increasing the magnetic field intensity had a negative effect on recovery, because gangue minerals enter into the magnetic separation concentrate under these conditions, resulting in a decreased iron grade of the magnetic separation concentrate.

The optimal conditions are as follows: roasting at 850 °C for 13 min with 15% coal ratio, grinding fineness of 80% less than 0.045 mm, and magnetic field intensity of 1200 Gs. Under these conditions, the iron and P_2O_5 contents of magnetic concentrate are 57.49% and 1.4%, respectively, with an iron recovery of 87.5% and a dephosphorization rate of 34.27%. It can be seen that it is difficult to obtain a good iron upgrading and dephosphorizing effect by using conventional magnetization roasting–magnetic separation.

3.2. Acid and Alkaline Leaching of Rough Magnetic Concentrate

3.2.1. Acid Leaching of the Rough Concentrate

Although the iron grade in the crude magnetite concentrate was 57.49%, the phosphorus content was still too high to meet the requirements of subsequent smelting. Therefore, a leaching experiment was conducted to further remove P from the rough concentrate. Apatite has good acid solubility, and the possible reactions during acid leaching are shown in Equations (4) and (5):





The effects of acid leaching parameters on the grade of iron and P_2O_5 and the iron recovery and dephosphorization rates of crude magnetite concentrate are presented in Figure 6. Figure 6a shows that the iron grade and dephosphorization rate increased from 59.82% to 60.53% and 25% to 85%, respectively, with increased acid dosage from 25 to 150 kg/t. Meanwhile, the P_2O_5 content and iron recovery rate decreased from 1.05% to 0.21% and 80.84% to 71.07%, respectively, indicating that effective removal of phosphorus was achieved when more iron-bearing minerals were involved in the leaching process. Therefore, the recommended optimal acid dosage is 150 kg/t.

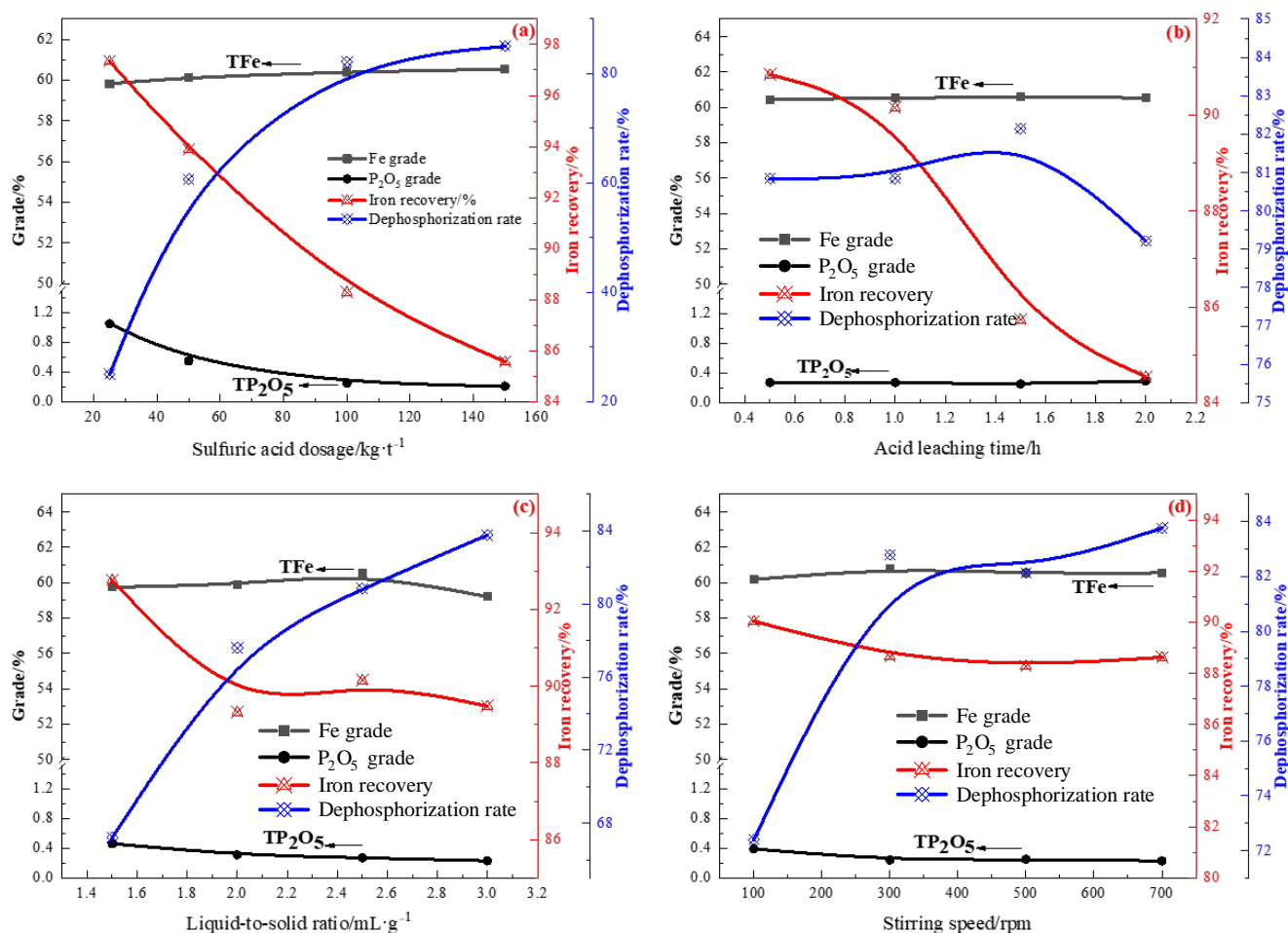


Figure 6. Effect of acid leaching parameters on the indices of rough iron concentrate leaching. (a) sulfuric acid dosage; (b) acid leaching time; (c) liquid-to-solid ratio; (d) stirring speed.

The effects of leaching time on the indices of rough iron concentrate under the conditions of leaching at 25 °C with 150 kg/t sulfuric acid concentration are shown in Figure 6b. Iron recovery decreased from 90.84% to 84.54% when the duration was prolonged from 0.5 h to 2 h. Meanwhile, the iron grade, P_2O_5 content, and dephosphorization rate changed slightly demonstrating that the dephosphorization reactions were almost completed within 0.5 h. From the above, acid leaching at 25 °C for 1 h is recommended, with the iron ore concentrate manufactured with 60.54% iron grade and 0.27% P_2O_5 grade at a recovery rate of 90.15% and a dephosphorization rate of 80.84%.

The effect of the solid-to-liquid ratio on the indices of rough iron concentrate leaching is presented in Figure 6c. The dephosphorization rate increased from 67.21% to 80.84% when the solid-to-liquid ratio was decreased from 0.67 g/mL to 0.4 g/mL. This is because the acid concentration increases with a decreased solid-to-liquid ratio, which is conducive to the solubility of phosphorus-bearing minerals. Further decreasing the solid-to-liquid

ratio has a negative impact on the iron grade and iron recovery. Therefore, the suggested optimal solid-to-liquid ratio is 0.4 g/mL.

The dephosphorization rate increased from 72.40% to 82.79% with increased stirring speed from 100 rpm to 300 rpm. Meanwhile, the P_2O_5 content decreased from 0.39% to 0.24%. When the stirring speed was increased further, the dephosphorization rate and P_2O_5 content changed slightly (Figure 6d). This is because a faster stirring speed can promote the diffusion rate of the solid–liquid surface reaction in the acid leaching process, resulting in an increased solution rate of iron- and phosphorus-bearing minerals [33]. Therefore, 300 rpm is recommended as the optimal stirring speed, with the grade of iron and P_2O_5 in the concentrate at 60.81% and 0.24%, respectively.

3.2.2. Alkaline Leaching of the Leached Concentrate

The iron grade of the concentrate obtained by the acid leaching process was only 60.81%, and there were still large amounts of aluminum and silicon minerals. Removing aluminum and silica gangue can help to upgrade the iron grade. Therefore, the alkaline leaching process was used to treat the leached concentrate with acid.

The grade of iron increased from 61.83% to 62.82% with increased alkaline dosage from 25 kg/t to 100 kg/t, as shown in Figure 7a. Meanwhile, the P_2O_5 content decreased from 0.213% to 0.124%. Further increasing the alkaline dosage had a slight effect on the indices. Therefore, the recommended optimal alkaline dosage is 100 kg/t. Figure 7b shows the effect of alkaline leaching time on the indices of the combined leaching process. The iron grade and dephosphorization rate increased when leaching time was extended from 0.5 h to 1 h. The indices changed slightly when the time was prolonged to 2 h. Therefore, the recommended optimal alkaline time is 1 h.

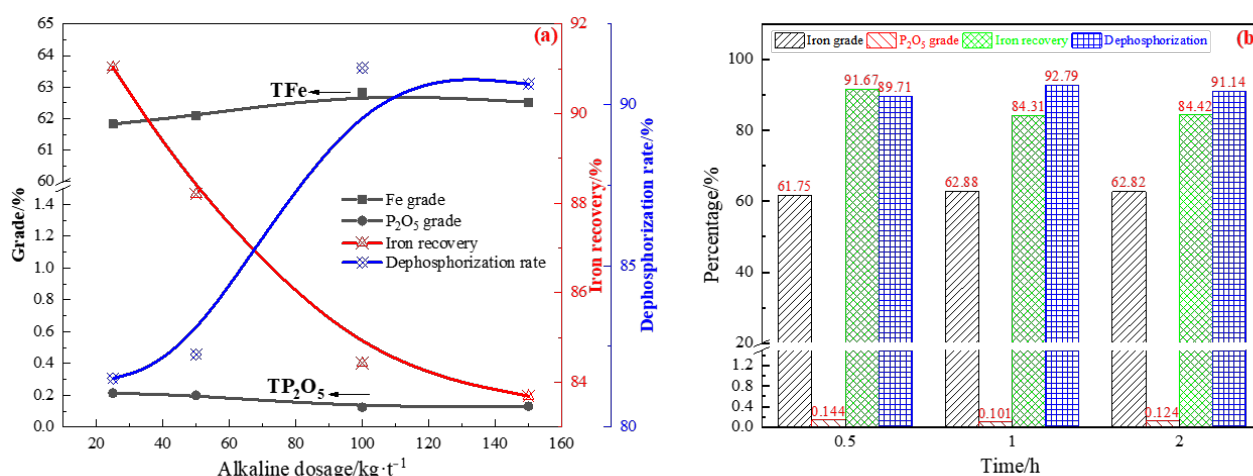


Figure 7. Effect of alkaline leaching parameters on the upgrade of iron and removal of phosphorus (a) alkaline dosage; (b) alkaline leaching time.

3.3. Sodium Magnetization Roasting

The effect of NaOH dosage on the indices of iron concentrate by magnetization–magnetic separation–acid/alkaline leaching is presented in Figure 8. The iron grade and P_2O_5 content in the concentrate increased from 62.88% to 70.21% and 0.101% to 0.185%, respectively, when NaOH was increased from 0 to 10%. Meanwhile, the dephosphorization rate decreased from 92.79% to 86.79%. Iron recovery increased from 84.31% to 85.47% when the NaOH dosage was increased from 0% to 2%. Further increasing the dosage had a negative effect on the index. Considering the cost and separation results, 2% NaOH is recommended as the optimal dosage. Al and some Si mostly exist in oolitic chlorite, mainly in a concentric ring structure closely embedded with iron minerals that are difficult to separate, as shown in Figure 3. Through the process of sodium magnetization roasting, part of the aluminum in iron minerals is transformed into sodium aluminosilicate or sodium

meta-aluminate, which reacts with dilute sulfuric acid into the solution in the process of acid leaching, achieving the purpose of dealumination [34]. At the same time, during the process of sodium magnetization roasting, SiO_2 changes into sodium silicate, which can react with dilute sulfuric acid. After that, the sodium silicate can react with dilute sulfuric acid to form silicic acid, which is removed in the process of filtration and water washing to realize the separation of Si and Fe. After adding NaOH, the following reactions can occur, as shown in Equations (6)–(11):

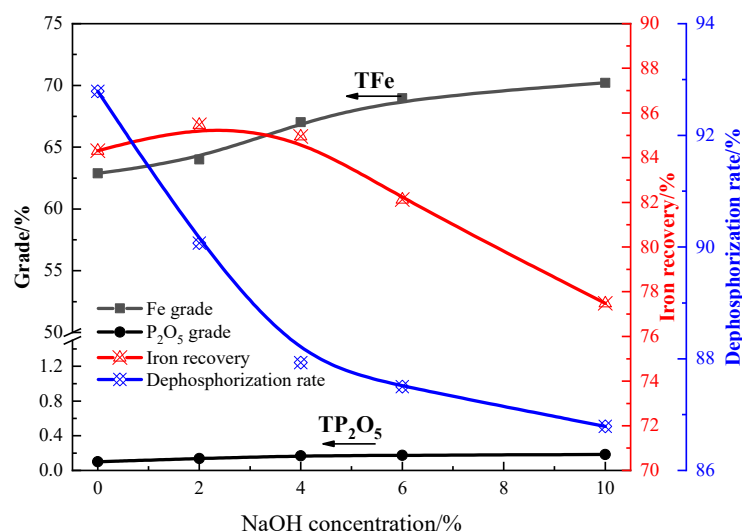
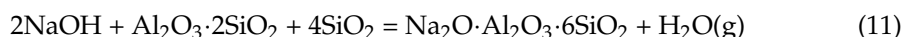
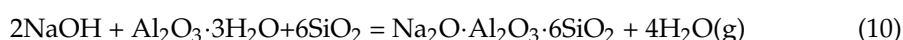
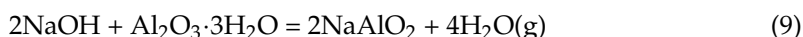
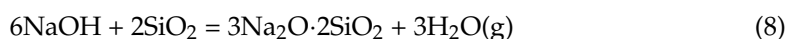
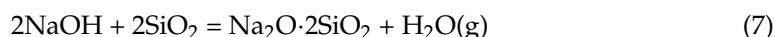
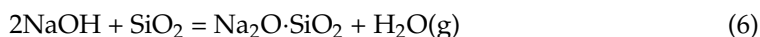


Figure 8. Effect of NaOH concentration on the indices of iron ore concentrate.

The ΔG_T – T relation of the above reactions (Equations (6)–(11)) can be obtained, and the initial reaction temperature is when $\Delta G_T = 0$, as shown in Table 3 and Figure 9.

Table 3. Reaction of ΔG_T – T relationship in the system with the addition of NaOH.

Equation	Relation of ΔG_T – T (J·mol ^{−1})	Temperature Range (K)	Initial Reaction Temperature (K)
(6)	$\Delta G_T = 72,609 - 140.985T$	298~1000	515.01
(7)	$\Delta G_T = 89,097 - 180.216T$	298~1000	494.39
(8)	$\Delta G_T = 109,180 - 110.007T$	298~1000	992.48
(9)	$\Delta G_T = 71,977 - 123.169T$	298~1000	584.38
(10)	$\Delta G_T = 201,633 - 421.170T$	298~1000	478.74
(11)	$\Delta G_T = 64,297 - 152.206T$	298~1000	422.43

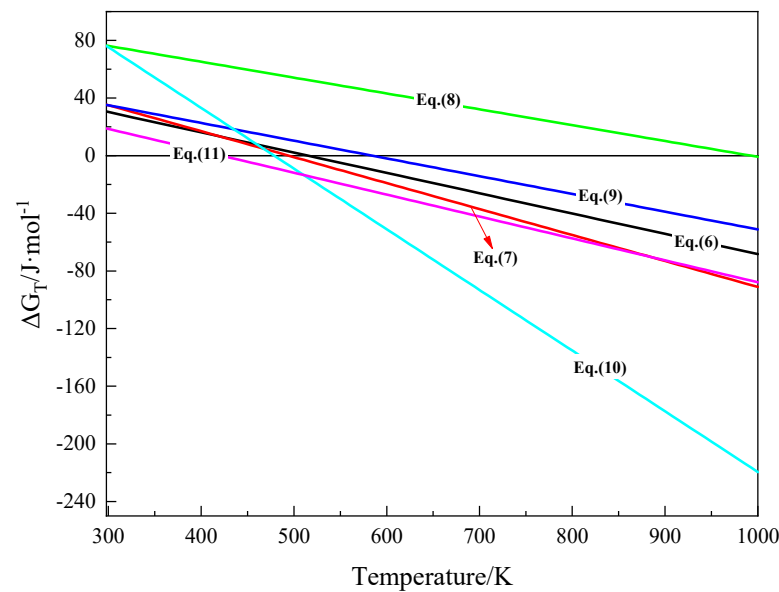


Figure 9. Reaction ΔG_T – T diagrams in the system with the addition of NaOH.

The XRD patterns of iron ore concentrates obtained at different NaOH dosages are shown in Figure 10. The main phases in the concentrate without NaOH are hematite, magnetite, and quartz. With an increase in the NaOH dosage, the quartz peak disappears.

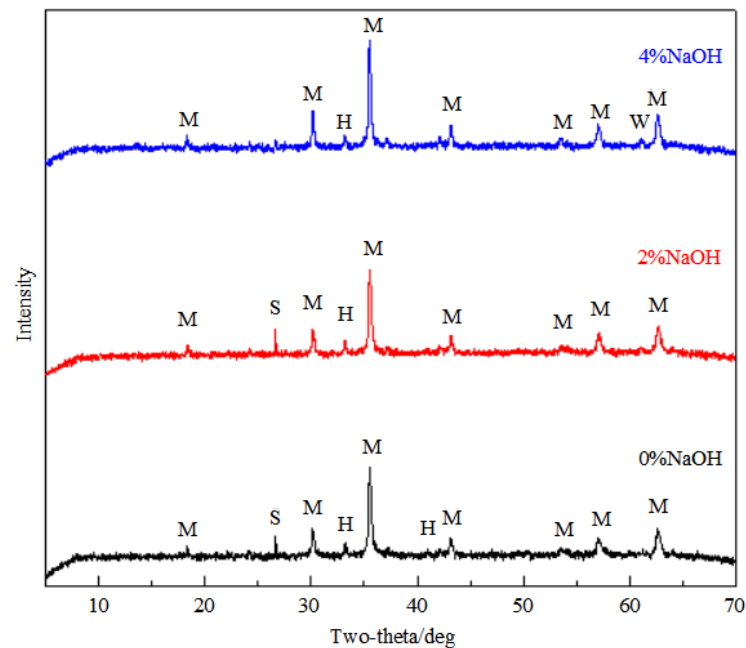


Figure 10. XRD patterns of iron ore concentrate obtained at different NaOH dosages. H, hematite; M, magnetite; S, quartz.

Figure 11 shows the enrichment of different elements under different NaOH dosages. Without adding NaOH, magnetic separation has a significant impact on iron upgrading. The iron grade in roasting–magnetic separation changed slightly when NaOH was added; the iron grade in the iron concentrate increased from 62.88% to 68.96% when NaOH was increased from 0% to 6% (Figure 11a). This is because a large number of aluminum- and silicon-bearing minerals are removed in the leaching process. Figure 11b shows that the Al_2O_3 content in raw ore and iron concentrate was 5.61% and 5.04%, respectively, without NaOH added, indicating that the removal of Al_2O_3 is limited. This is because most of

the aluminum exists in the chamosite, which is closely embedded with iron minerals and difficult to separate. Part of the aluminum transforms to sodium aluminosilicate or sodium aluminate when NaOH is added, which can be removed in the leaching process. Figure 11c shows the enrichment of silicon under different NaOH dosages. In the absence of NaOH, the desiliconization process mainly reacts in the magnetic separation process. The desiliconization rate increased from 58% to 92% with increased NaOH dosage from 0% to 6%, indicating that the silicon-bearing minerals transformed to sodium aluminosilicate or sodium silicate in the process of roasting with NaOH, which agrees with the thermodynamic calculation. Whether NaOH is added or not, the dephosphorization reaction mainly occurs in the acid leaching process, as seen in Figure 11d.

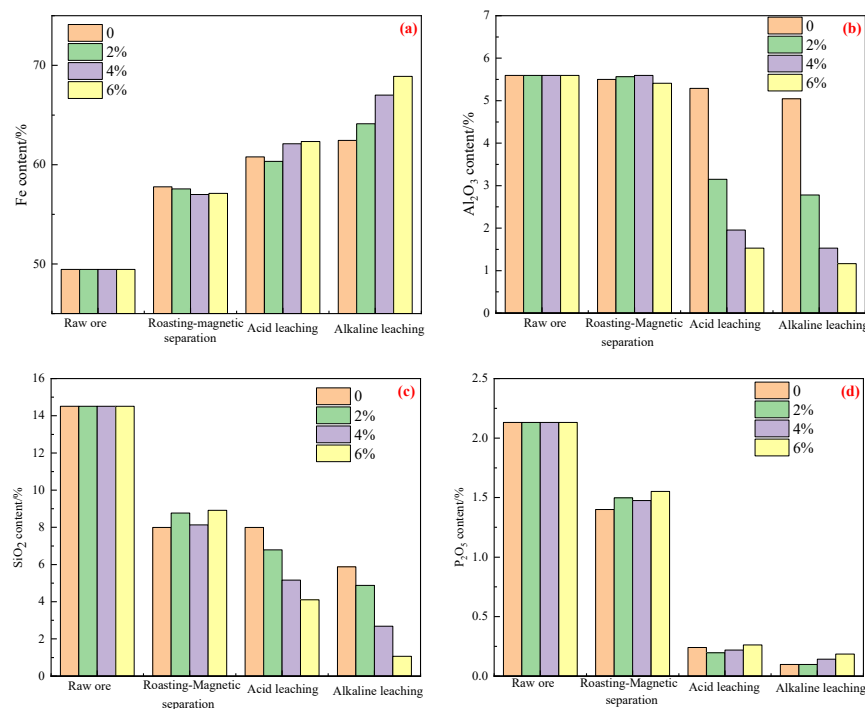


Figure 11. Enrichment of different elements in the concentrate under different NaOH dosages at different stages of beneficiation. (a) Fe content; (b) Al_2O_3 content; (c) SiO_2 content; (d) P_2O_5 content.

Considering that when 2% NaOH was added, the P_2O_5 in the concentrate was still a little high, some measures such as adjusting the roasting duration and the alkaline leaching conditions were taken to improve the chemical compositions. Figure 12 presents the effects of roasting duration and alkaline leaching conditions on the indices. As shown in Figure 12a, the dephosphorization rate increased from 90.21% to 91.79% with prolonged roasting duration from 11 min to 17 min. Meanwhile, the iron recovery rate decreased slightly from 85.38% to 84.64%. The change of roasting duration had a slight impact on the iron grade and P_2O_5 content in the iron concentrate, but when the duration was only 13–15 min, the iron grade reached more than 64%. Therefore, roasting for 15 min is recommended, with the iron concentrate manufactured with a grade of 64.03% Fe_{total} and 0.128% of P_2O_5 at an iron recovery rate of 85.42% and a dephosphorization rate of 90.86%.

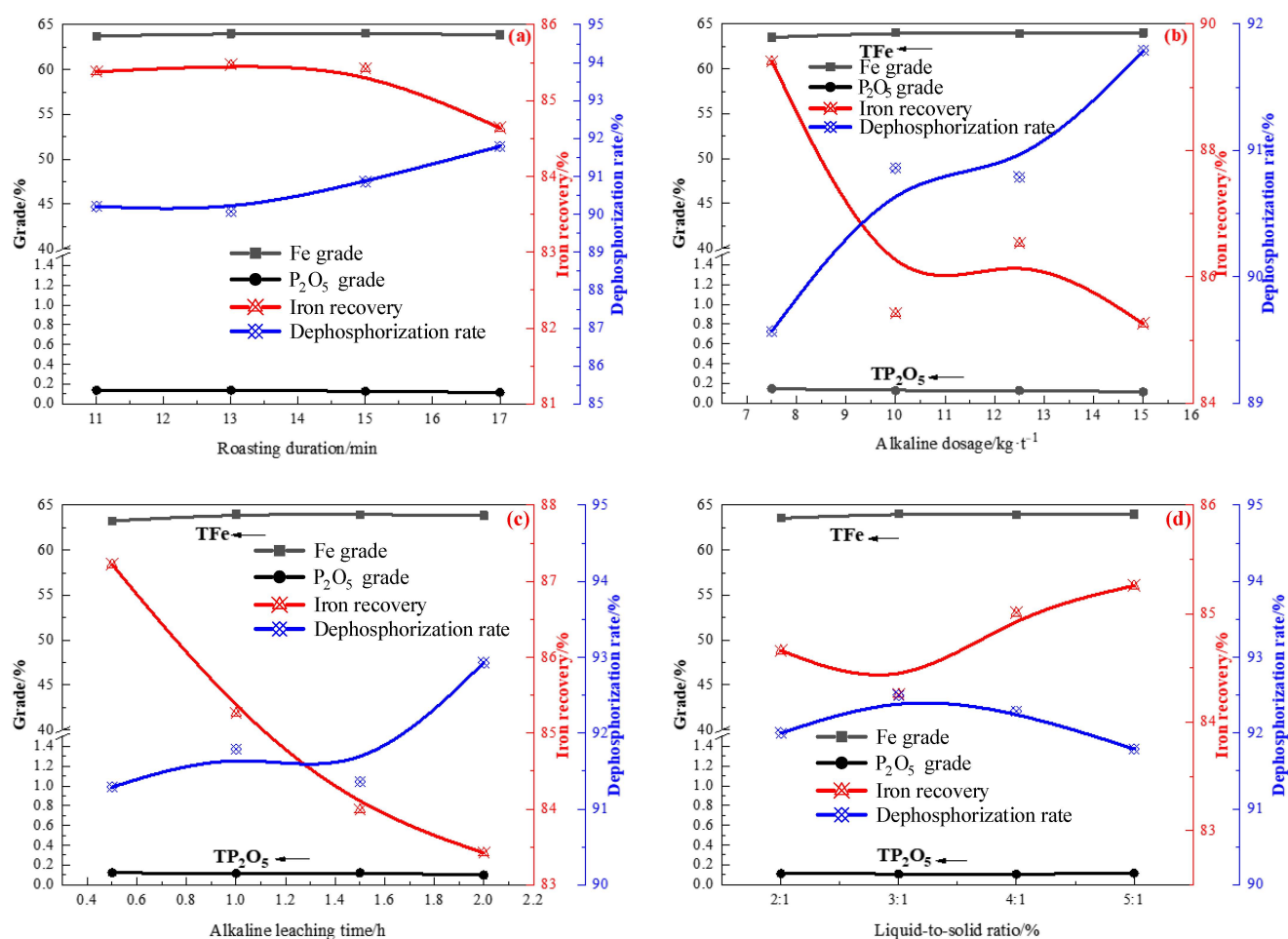


Figure 12. Effects of roasting duration and alkaline leaching conditions on the indices. (a) roasting duration; (b) alkaline dosage; (c) alkaline leaching time; (d) liquid-to-solid ratio.

Figure 12b presents the effects of alkaline dosage on the indices of the iron ore concentrate. The grade of iron and P₂O₅ content changed slightly when the alkaline dosage was increased from 75 to 150 kg/t. However, the iron recovery decreased from 89.41% to 85.26% and the dephosphorization rate increased from 89.57% to 91.79%, indicating that the NaOH reacts with apatite wrapped in aluminum- and silica-bearing gangue minerals to form hydrated sodium phosphate, which is easily soluble in water. Considering the grade of iron and dephosphorization rate, the suggested optimal alkaline dosage is 150 kg/t.

Figure 12c presents the increased iron grade from 63.25% to 64.01% with increased leaching time from 0.5 to 1 h. Further prolonging the duration had a slight effect on the iron grade. However, iron recovery decreased from 87.22% to 83.42%. Meanwhile, the P₂O₅ content decreased from 0.122% to 0.099%. Therefore, the optimal leaching time is recommended as 1 h.

It can be seen from Figure 12d that the iron grade increased from 63.55% to 64.07% when the liquid-to-solid ratio was increased from two to three. Further increasing the liquid-to-solid ratio had a slight impact on the iron grade. Therefore, the optimal liquid-to-solid ratio is 3 mL/g, with the iron concentrate manufactured with 64.07% iron grade and 0.108% P₂O₅ grade at a recovery rate of 84.26% and a dephosphorization rate of 92.50%.

3.4. Characterization of the Iron Ore Concentrate

Table 4 shows the chemical compositions of the final iron concentrate by the sodium magnetization roasting–acid leaching–alkaline leaching process under the optimum conditions described above. It can be seen that the iron grade was 64.11%, and the contents of Al_2O_3 , SiO_2 , and P_2O_5 were only 2.79%, 4.90%, and 0.097%, respectively, so it is a good quality concentrate. This new process is an effective technique to enrich iron and remove phosphorus from high-phosphorus oolitic iron ore. Figure 13 presents the SEM-EDS results of iron concentrate. It can be seen that the purity of magnetite in the iron concentrate was relatively high, and there were only two elements of Fe and O at point 1, which is pure magnetite. No separate aluminum-bearing minerals existed in the iron concentrate. A small amount of aluminum was detected at points 3 and 4; this part of aluminum exists in the form of isomorphism in iron minerals and is difficult to remove. Silicon mainly occurs in the form of quartz in the iron concentrate such as at point 2. This part of the quartz cannot be removed due to the fine particle size or because it is wrapped by iron minerals, and it remains in the final iron concentrate.

Table 4. Chemical compositions of the final ore iron concentrate (wt.%).

Element	TFe	FeO	CaO	MgO	SiO ₂	Al ₂ O ₃	Na ₂ O	S	P ₂ O ₅
Concentrate	64.11	34.63	0.81	0.03	4.90	2.79	0.06	0.10	0.097

The distribution of phosphorus in the iron ore concentrate is shown in Figure 14. The remaining phosphorus-bearing minerals in the concentrate were all apatite, with a particle size below 10 μm . The apatite is completely encased in the iron mineral (point 1), which is difficult to separate from iron by physical magnetic separation or chemical reaction. Due to the close inlay of apatite and iron mineral (point 2), even if the iron mineral is partially destroyed, the apatite is difficult to remove. The phosphorus-bearing mineral (point 3) is not encased by the iron mineral; it contains 4.27% fluorine and is fluorapatite. Compared with hydroxyapatite, the crystal structure of the mineral changes due to the replacement of OH^- by F^- . F^- and Ca^{2+} can form a F–Ca bond, which has a shorter bond length, higher bond energy, and stronger binding effect. Therefore, fluorapatite is more stable than hydroxyapatite.

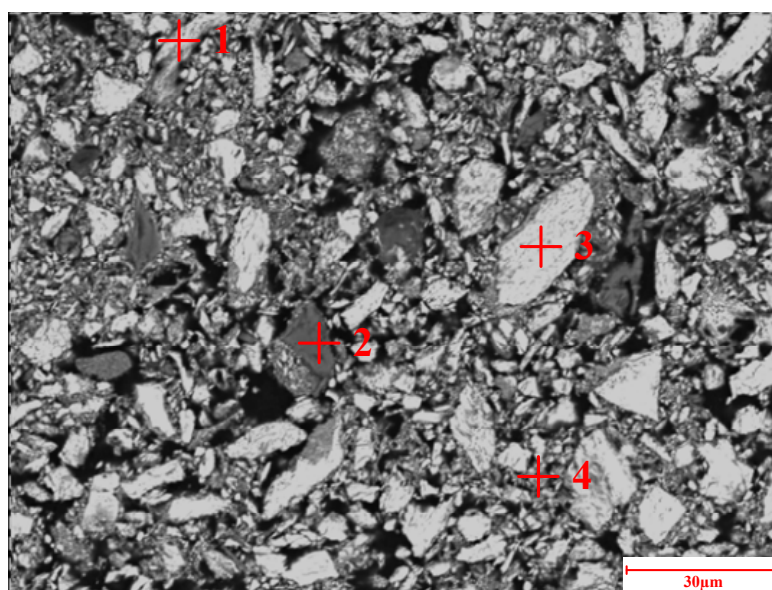


Figure 13. *Cont.*

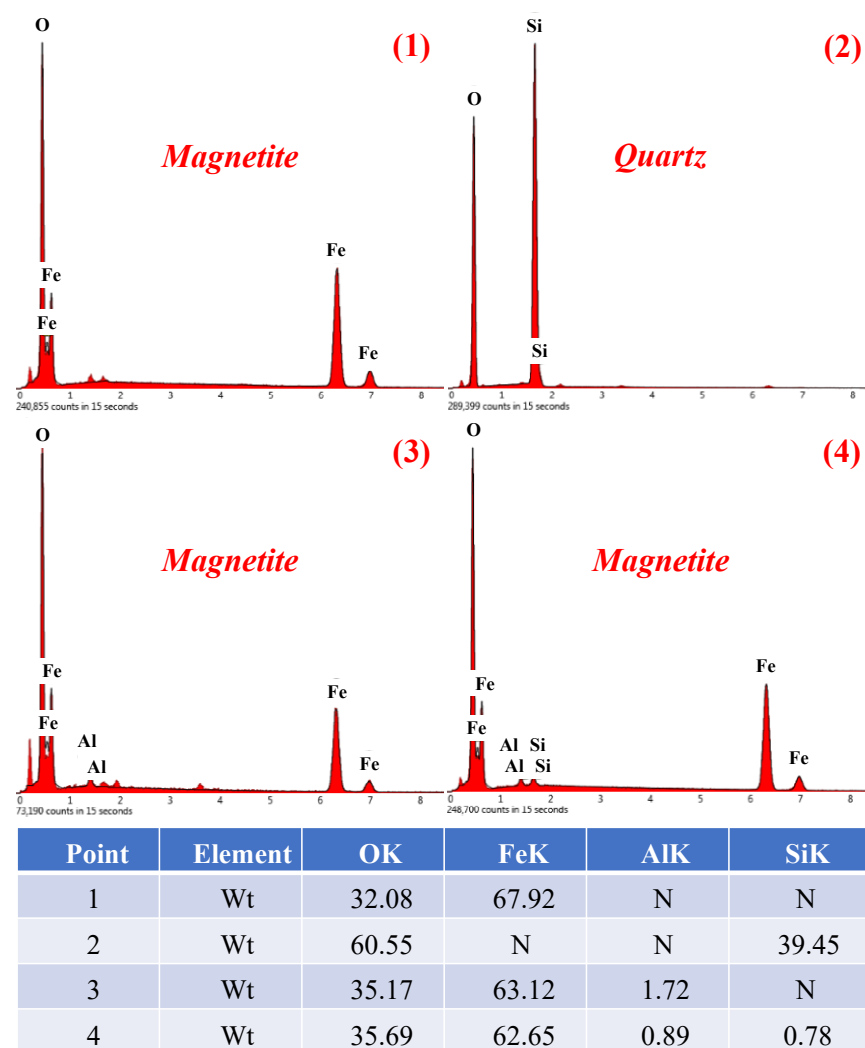


Figure 13. SEM-EDS results of the iron ore concentrate.

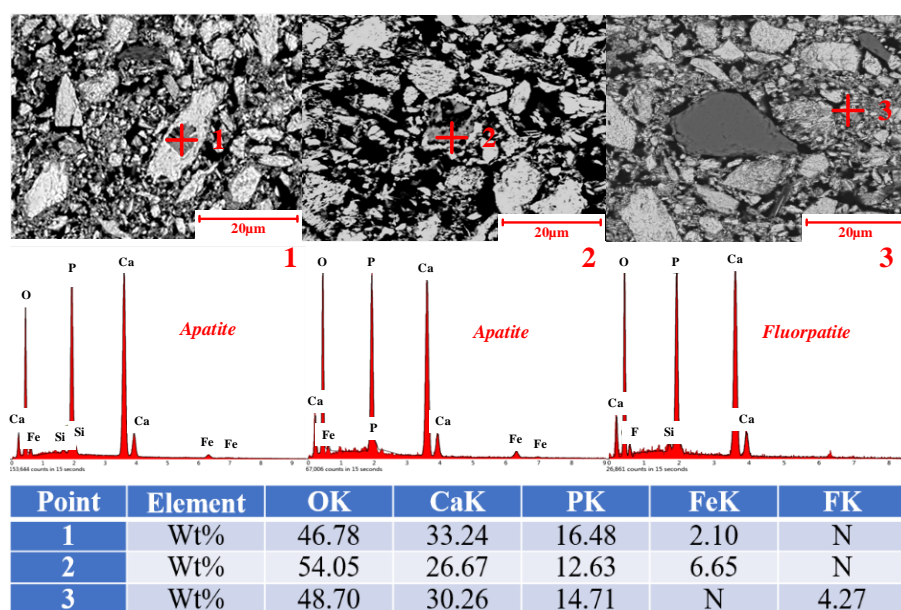


Figure 14. Distribution of phosphorus in the iron ore concentrate.

4. Conclusions

A new method of upgrading a high-phosphorus oolitic hematite by sodium magnetization roasting–magnetic separation–leaching was developed, and the main conclusions can be drawn as follows:

- (1) High-phosphorus oolitic hematite ore containing 49.41% Fe and 2.13% P_2O_5 was used as a raw material. Magnetization roasting–magnetic separation was used to treat this ore under optimized conditions of roasting at 850 °C for 13 min with 10% coal. The roasted briquettes were subjected to wet magnetic separation under conditions of grinding fineness of 80% less than 0.045 mm and magnetic field intensity of 1200 Gs, and the rough magnetic separation concentrate contained 57.49% Fe and 1.4% P_2O_5 , with an iron recovery rate of 87.5% and a dephosphorization rate of 34.27%. Conventional magnetization roasting could not significantly change the mineral embedding relationship in oolitic hematite ore. Magnetic separation could only separate part of the coarse gangue minerals, and there was no targeted treatment of P, indicating that it is difficult to upgrade iron and phosphorus removal by the conventional magnetization roasting–magnetic separation process.
- (2) Acid leaching was performed to remove phosphorus from the rough magnetic separation concentrate. Under optimal conditions, the final product (acid leaching residue), assayed at 60.81% Fe and 0.24% P_2O_5 , was produced at an iron recovery rate of 88.66% and dephosphorization rate of 82.79%. It was found that acid leaching had a certain effect on removing phosphorus. However, the P_2O_5 content in the iron concentrate was still high, implying that a small part of P does not occur in the form of apatite. Therefore, an alkaline leaching process was used to treat the acid leaching residue. Under conditions of NaOH concentration of 100 kg/t and reaction at 90 °C for 1 h with a liquid-to-solid ratio of 5 and stirring speed of 500 rpm, the iron concentrate contained 62.88% iron and 0.101% P_2O_5 . Due to the strong alkalinity of sodium hydroxide, it can further react with undeleted aluminum and silica gangue minerals in the process of alkali leaching to produce water-soluble sodium silicate and sodium meta-aluminate, which can be removed during slag liquid separation. Compared with the iron ore concentrate assayed at 57.49% Fe and 1.4% P_2O_5 , the final concentrate by the new process, assayed at 64.11% Fe, with an iron recovery of 67.03% and 0.097% P_2O_5 with a dephosphorization rate of 95.45%, was successfully manufactured.
- (3) NaOH can participate in reactions with aluminum- and silica-bearing minerals during the magnetization roasting process, intensifying the removal of these minerals in the acid and alkaline leaching processes. For roasting, 4–6% NaOH was added to the ore, resulting in a higher iron grade and lower SiO_2 , Al_2O_3 , and P_2O_5 . Sodium magnetization roasting is very effective at transferring hematite into magnetite, and aluminum- and silica-bearing minerals into soluble sodium compounds.

Author Contributions: Conceptualization, J.P. and D.Z.; Data curation, S.L. (Shenghu Lu) and T.D.; Formal analysis, S.L. (Shenghu Lu) and Z.G.; Funding acquisition, J.P. and D.Z.; Investigation, J.P. and S.L. (Siwei Li); Methodology, S.L. (Siwei Li) and D.Z.; Project administration, S.L. (Shenghu Lu); Resources, J.P. and D.Z.; Software, Y.S.; Supervision, Z.G.; Validation, D.Z. and T.D.; Visualization, Y.S.; Writing—original draft, S.L. (Shenghu Lu) and S.L. (Siwei Li); Writing—review & editing, J.P. and D.Z. All authors have read and agreed to the published version of the manuscript.

Funding: Natural Science Foundation of China (No. 51474161); Fundamental Research Funds for the Central Universities of Central South University (No. 2021zzts0291); Innovation-driven Project of Guangxi Zhuang Autonomous Region (No. AA18242003); and the Innovation-driven Project of Guangxi Zhuang Autonomous Region (No. AA148242003).

Acknowledgments: The authors wish to express their thanks to the National Natural Science Foundation of China (No. 51474161) and Innovation-driven Project of Guangxi Zhuang Autonomous Region (No. AA18242003, No. AA148242003). The work was financially supported by the Fundamental Research Funds for the Central Universities of Central South University (No. 2021zzts0291).

Conflicts of Interest: The authors declare no conflict of interest.

References

- Li, G.H.; Zhang, S.H. Effects of sodium salts on reduction roasting and Fe-P separation of high-phosphorus oolitic hematite ore. *Int. J. Miner. Processing* **2013**, *124*, 26–34. [\[CrossRef\]](#)
- Rao, M.J.; Ouyang, C.X. Behavior of phosphorus during the carbothermic reduction of phosphorus-rich oolitic hematite ore in the presence of Na₂SO₄. *Int. J. Miner. Processing* **2015**, *143*, 72–79. [\[CrossRef\]](#)
- Mcgregor, F.; Ramanaidou, E. Phanerozoic ooidal ironstone deposits—generation of potential exploration targets. *Appl. Earth Sci.* **2010**, *119*, 60–64. [\[CrossRef\]](#)
- Baioumy, H.; Omran, M. Mineralogy, geochemistry and the origin of high-phosphorus oolitic iron ores of Aswan, Egypt. *Ore Geol. Rev.* **2017**, *80*, 185–199. [\[CrossRef\]](#)
- Li, G.F.; Han, Y.X. Enrichment of phosphorus in reduced iron during coal based reduction of high phosphorus-containing oolitic hematite ore. *Ironmak. Steelmak.* **2016**, *43*, 163–170. [\[CrossRef\]](#)
- Luo, L.Q.; Zhang, H.Q. Process mineralogy and characteristic associations of iron and phosphorus-based minerals on oolitic hematite. *J. Cent. South Univ.* **2017**, *24*, 1959–1967. [\[CrossRef\]](#)
- Rao, Z.Q.; Zhang, Y.S. Improved Flotation of Oolitic Hematite Ore Based on a Novel Cationic Collector. *Adv. Mater. Res.* **2013**, *712*, 743–747. [\[CrossRef\]](#)
- Muhammed, M.; Zhang, Y. A hydrometallurgical process for the dephosphorization of iron ore. *Hydrometallurgy* **1989**, *21*, 277–292. [\[CrossRef\]](#)
- Ionkov, K.; Gaydardzhiev, S. Dephosphorisation of limonitic concentrate by roasting, acid leaching and magnetic separation. In Proceedings of the Iron Ore Conference 2011, Perth, Australia, 11–13 July 2011; pp. 445–452.
- Hanna, J.; Anazia, I.J. Processing of hematitic iron ores. In *Advances in Fine Particles Processing*; Springer: New York, NY, USA, 1990; pp. 413–425.
- Omran, M.; Fabritius, T. Improvement of phosphorus removal from iron ore using combined microwave pretreatment and ultrasonic treatment. *Sep. Purif. Technol.* **2015**, *156*, 724–737. [\[CrossRef\]](#)
- Nunes, A.P.L.; Pinto, C.L.L. Floatability studies of wavellite and preliminary results on phosphorus removal from a Brazilian iron ore by froth flotation. *Miner. Eng.* **2012**, *39*, 206–212. [\[CrossRef\]](#)
- Zhang, Y.; Muhammed, M. An integrated process for the treatment of apatite obtained from dephosphorization of iron ore. *J. Chem. Technol. Biotechnol.* **2010**, *47*, 47–60. [\[CrossRef\]](#)
- Xia, W.T.; Ren, Z.D. Removal of Phosphorus from High Phosphorus Iron Ores by Selective HCl Leaching Method. *J. Iron Steel Res. Int.* **2011**, *18*, 1–4. [\[CrossRef\]](#)
- Ionkov, K.; Gaydardzhiev, S. Amenability for processing of oolitic iron ore concentrate for phosphorus removal. *Miner. Eng.* **2013**, *46*, 119–127. [\[CrossRef\]](#)
- Delvasto, P.; Ballester, A. Mobilization of phosphorus from iron ore by the bacterium *Burkholderia caribensis* FeGL03. *Miner. Eng.* **2009**, *22*, 1–9. [\[CrossRef\]](#)
- Wang, J.C.; Shen, S.B. Effect of ore solid concentration on the bioleaching of phosphorus from high-phosphorus iron ores using indigenous sulfur-oxidizing bacteria from municipal wastewater. *Process Biochem.* **2010**, *45*, 1624–1631. [\[CrossRef\]](#)
- Delvasto, P.; Valverde, A. Diversity and activity of phosphate bioleaching bacteria from a high-phosphorus iron ore. *Hydrometallurgy* **2008**, *92*, 124–129. [\[CrossRef\]](#)
- Matinde, E.; Hino, M. Dephosphorization Treatment of High Phosphorus Iron Ore by Pre-reduction, Mechanical Crushing and Screening Methods. *ISIJ Int.* **2011**, *51*, 220–227. [\[CrossRef\]](#)
- Matinde, E.; Hino, M. Dephosphorization Treatment of High Phosphorus Iron Ore by Pre-reduction, Air jet Milling and Screening Methods. *ISIJ Int.* **2011**, *51*, 544–551. [\[CrossRef\]](#)
- Wu, J.; Wen, Z.J. Development of Technologies for High Phosphorus Oolitic Hematite Utilization. *Steel Res. Int.* **2011**, *82*, 494–500.
- Sun, Y.S.; Han, Y.X. Recovery of iron from high phosphorus oolitic iron ore using coal-based reduction followed by magnetic separation. *Int. J. Miner. Metall. Mater.* **2013**, *20*, 411–419. [\[CrossRef\]](#)
- Yu, W.; Sun, T. Can sodium sulfate be used as an additive for the reduction roasting of high-phosphorus oolitic hematite ore? *Int. J. Miner. Processing* **2014**, *133*, 119–122. [\[CrossRef\]](#)
- Zhu, D.Q.; Guo, Z.Q. Synchronous Upgrading Iron and Phosphorus Removal from High Phosphorus Oolitic Hematite Ore by High Temperature Flash Reduction. *Metals* **2016**, *6*, 123. [\[CrossRef\]](#)
- Yang, C.C.; Zhu, D.Q. Simultaneous Recovery of Iron and Phosphorus from a High-Phosphorus Oolitic Iron Ore to Prepare Fe-P Alloy for High-Phosphorus Steel Production. *JOM* **2017**, *69*, 1663–1668. [\[CrossRef\]](#)
- Li, S.W.; Pan, J. Synchronous enrichment of phosphorus and iron from a high-phosphorus oolitic hematite ore to prepare Fe-P alloy by direct reduction-magnetic separation process. *J. Cent. South Univ.* **2021**, *28*, 2724–2734. [\[CrossRef\]](#)
- Kokal, H.; Singh, M. Removal of phosphorus from Lisakovsky iron ore by a roast-leach process. *Electrometall. Environ. Hydrometall.* **2013**, *2*, 1517–1541.
- Xu, C.Y.; Sun, T.C. Mechanism of phosphorus removal in beneficiation of high phosphorous oolitic hematite by direct reduction roasting with dephosphorization agent. *Trans. Nonferrous Met. Soc. China* **2012**, *22*, 2806–2812. [\[CrossRef\]](#)

-
29. Ionkov, K.; Gomes, O.; Neumann, R. Process Oriented Characterization of Oolitic Iron Concentrate during Dephosphorisation by Roasting and Leaching. In Proceedings of the IMPC 2016: XXVIII International Mineral Processing Congress, Quebec City, QC, Canada, 11–15 September 2016.
 30. Li, S.W.; Pan, J. A novel process to upgrade the copper slag by direct reduction-magnetic separation with the addition of Na_2CO_3 and CaO. *Powder Technol.* **2019**, *347*, 159–169. [[CrossRef](#)]
 31. Wang, D.Z.; Zhu, D.Q. A high-efficiency separation process of Fe and Zn from zinc-bearing dust by direct reduction. *J. Iron Steel Res. Int.* **2022**, *14*. [[CrossRef](#)]
 32. Xue, Y.X.; Pan, J. Improving High-Alumina Iron Ores Processing via the Investigation of the Influence of Alumina Concentration and Type on High-Temperature Characteristics. *Minerals* **2020**, *10*, 802. [[CrossRef](#)]
 33. Cekinski, E.; Thomassin, J.H. Surface Investigation of the Reaction Products between Apatite and Sulfuric Acid. *Phosphorus Sulfur Silicon Relat. Elem.* **1993**, *76*, 235–238. [[CrossRef](#)]
 34. Wang, D.Z.; Zhu, D.Q. An Investigation into the Alkali Metals Removal from Zn-Bearing Dust Pellets in Direct Reduction. *JOM* **2022**, *74*, 634–643. [[CrossRef](#)]